3 Molecular Interactions-Assisted Grading of Polymers for the Development of Stable Amorphous Solid Dispersion of Riluzole

3.1 Background of the study

The development of a stable ASD requires understanding of the mechanistic insight of drug's interaction with polymers in terms of T_g, drug de-mixing, drug-polymer miscibility, phase solubility of drugs in polymer matrix, physical stability of drug, and preparation process.

3.1.1 Plan of work

The current study involves a detailed study to comprehend the drug-polymer interactions in the formulation of a kinetically and thermodynamically stable ASD of RLZ.

i) Initial screening of the suitable polymers for ASD preparation and understanding the molecular level interactions were carried out by extensive *in silico* studies.

ii) The experimental validation of the results was done by powder X-ray diffraction (PXRD), differential scanning calorimetry (DSC), fourier transform infrared spectroscopy (FT-IR), solid-state NMR (ssNMR), microscopic analysis by using scanning electron microscopy (SEM) and transmission electron microscopy (TEM). Mathematical modeling using Flory-Huggins theory was also used to determine the extent of drug loading and the temperature, up to which an ASD system will uphold its homogenous phase.

3.2 Experimental section

3.2.1 Methodology for in silico studies

3.2.1.1 Preparation of 3D Structures of Polymers

The 3D structures of polymers were designed using polymer builder tool in Macromodel module of Schrodinger software package [165]. Chain growth with backbone dihedral option was set to variable between 120-210 degrees to avoid clashes. The energy minimization of the models was performed on the single polymer chains using OPLS3 force field in vacuum using Powell-Reeves conjugate gradient (PRCG) method. The resultant optimized geometries of polymers were subjected to 20 ns of molecular dynamics simulations using Desmond module [166] of Schrodinger software package. The most stable forms of polymer chains were taken for further study. To design the polymers: PAA, PVP VA and HPMC AS, following monomeric compositions were considered based on the literature reports:

For polyacrylic acid PAA: 19 units of acrylic acid and one unit of acrylate allyl pentaerythreitol were used in a linear combination (AAAAAAAAAABAAAAAAAAA) to obtain a polymer of length equal to 20 units. The molecular weight of designed PAA polymer was 1600 with the chemical formula $C_{68}H_{96}O_{43}$. Figure 3.1a represents the general 2D structure of the polymer [167].

For PVP VA: Vinyl acetate and vinyl pyrrolidone were linked by linear random free-radical polymerization at 1:1 weight ratio (8:12 molar ratio, respectively) as shown in Figure 3.1b [168]. The molecular weight and formula for 20 monomers containing PVP VA were 1698 and $C_{80}H_{112}N_{10}O_{30}$, respectively.

For HPMC AS: Block copolymerization of 5 units of substituted cellulose was carried out in ABCAB sequence, wherein A represents the cellulose unit with two acetyl, three methoxy and one hydroxypropoxy substitutions in place of R. B represents the cellulose unit with two acetyl, two succinoyl and two methoxy substitutions. C represents the cellulose unit with two acetyl, two methoxy, one succinoyl and one hydroxypropoxy substitutions [169]. The general structure of HPMCAS is shown in Figure 3.1c. The designed HPMC AS had the molecular weight and chemical formula 2428 and $C_{102}H_{164}O_{65}$, respectively.

For RLZ: The chemical structure of RLZ is shown in Figure 3.1d. The initial crystal structure of RLZ was adopted from Cambridge Crystallographic Data Centre (CSD Deposition number: 1820861). The coordinates of the 3D structure of RLZ were obtained from the crystal structure using Mercury software. The same coordinates were used to generate 3D model of RLZ for further computational calculations.

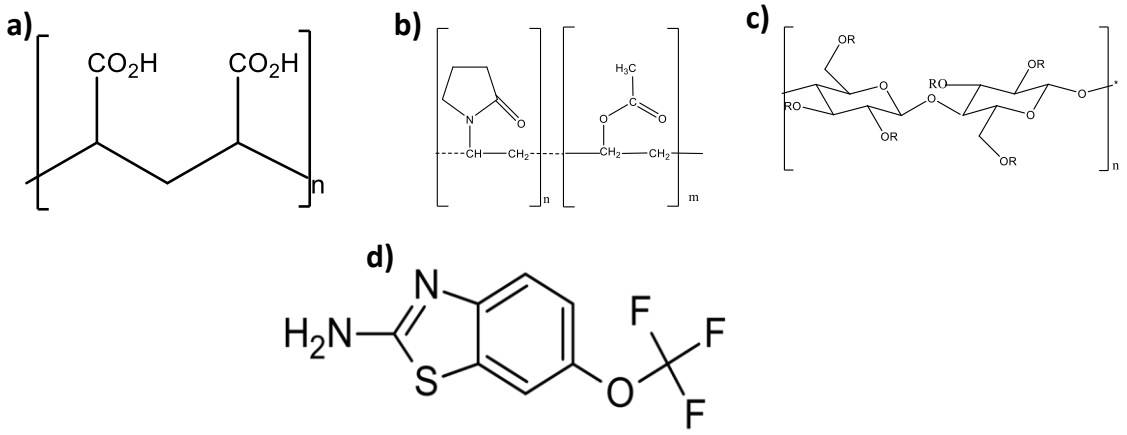

Figure 3.1. General structural representation of the monomeric units of a) PAA, b) PVP VA, c) HPMC AS, and d) RLZ.

3.2.1.2 Molecular docking

Molecular docking analysis of RLZ on designed polymers was done using Glide module of Schrodinger software package [170]. RLZ was docked at multiple sites of the polymers

to obtain the best possible sites of interactions and binding affinity of the drug-polymer complexes.

3.2.1.3 Molecular dynamics simulations (MDS):

MDS were carried out using Desmond module of Schrodinger package. Systems were built in vacuum using orthorhombic box with buffer size of 10 Å buffer from all the sides using OPLS3 force field. Simulations were run using NPT ensemble at 300 K temperature. Polymers were simulated for 20 ns at 2 ps record interval and 8ps trajectory. The drug-polymer complexes were simulated for 40 ns at 2 ps record interval and 8ps trajectory.

3.2.1.4 Density functional theory (DFT) calculations

DFT calculations were performed using Gaussian09 program suite [171] to obtain the drug-polymer interaction energies in the complexes. The 3D geometries of the three polymers were optimized at semi empirical PM6 level of theory [172] and the 3D structure of RLZ molecule was optimized at B3LYP/6-31+G(d,p) level of theory [173]. RLZ-polymer complex was optimized using ONIOM (Our own n-layered Integrated molecular Orbital and Molecular mechanics) method [174], wherein the polymer was optimized as low layer at semi-empirical PM6 level and RLZ was optimized as high layer at B3LYP/6-31+G(d,p) level. All the geometries were optimized in both gas phase and solvent phase using IEFPCM solvent model [175] and methanol (ε=32.7) as the implicit solvent. Since, methanol was used as the polar protic solvent to dissolve the RLZ and polymers in experimental conditions, it was the choice of solvent to study the effect of solvent on drug-polymer interaction energies. The interaction energies of drug-polymer complexes were calculated using the following formula:

$$\Delta E_{interaction} = E_{complex} - [E_{polymer} + E_{drug}]$$

Where $E_{complex}$, $E_{polymer}$ and E_{drug} are the Gibbs free energies of drug-polymer complex, polymer and drug respectively.

3.2.2 Development of amorphous solid dispersion of RLZ and physical mixtures of RLZ with polymers

For preliminary studies ASDs with different ratios of drug and polymers (Table 1) were prepared by rapid solvent evaporation method using rotary evaporator (IKA RV 10 auto pro V). The ASDs were prepared by taking RLZ and the polymers in the ratio mentioned in the Table 1. The solvent system of methanol:dichloromethane (1:1) was used as solvent to solubilize RLZ and the polymers to prepare uniform solutions. The resultant solution was subjected to vacuum evaporation with bath temperature set to 55 ^{o}C and gradually applying vacuum from 500 mBar to 2 mBar. The residual solvent was removed by drying the ASDs in vacuum oven at 25 ^{o}C for 24 hours. The samples were passed through ASTM #100 and stored over P_2O_5 until further analysis.

For physical mixture preparation different weight ratios of RLZ and each of the polymer were taken and geometrically mixed. Geometric mixing was done to avoid any kind of change in the solid form of the drug. RLZ was mixed in the composition of 95% w/w, 90% w/w, 85% w/w and 80% w/w with each of the polymer. For T_g determination, the physical mixtures were prepared with 90% w/w, 70% w/w and 50% w/w of RLZ with each of the polymer. The physical mixtures were stored over P_2O_5 until use.

Table 3.1. Composition details for the preparation of ASD with different polymers

S.No	Formulation Code	% w/w of Drug	Drug/Polymer
1	F1A	50	RLZ/PAA
2	F2A		RLZ/PVP VA
3	F3A		RLZ/HPMC AS
4	F1B	70	RLZ/PAA
5	F2B		RLZ/PVP VA
6	F3B		RLZ/HPMC AS

7	F1C	90	RLZ/PAA
8	F2C		RLZ/PVP VA
9	F3C		RLZ/HPMC AS

3.2.3 Powder X-ray diffraction study

Powder XRD study was done on benchtop Rigaku Miniflex 600 X-ray diffractometer to confirm the formation of ASDs prepared with different polymers and their different weight ratios. Analysis was carried out at 40 kV voltage, 15 mA current and Ni-filtered Cu-K radiation with 20 mm monochromator slit . The radiation scattered on the samples was measured with a vertical goniometer. X-ray diffraction patterns were obtained at the 2θ values ranging from of 5° to 50° at the scan speed of 5°/min with a step size of 0.02° [176].

3.2.4 Determination of melting point and glass transition temperature

The thermal behavior of physical mixtures of RLZ with PAA, PVP VA, HPMC AS and ASDs of RLZ prepared with these polymers were analyzed through DSC. The melting point of the pure crystalline RLZ was determined by observing the presence of endothermic peak when the ramp rate was set at 10^{o}C/min until 140 ^{o}C.

The physical mixtures in different composition (90% w/w, 70% w/w, 50% w/w of drug) were subjected to heat-cool-heat cycle in the DSC. Samples were heated till 140 ^{o}C, at a rate of 10 ^{o}C/min followed by cooling at a rate of 20 ^{o}C/min to 0 ^{o}C. From 0 ^{o}C onwards, the sample was reheated until 140 ^{o}C at the rate of 20 ^{o}C/min. The T_g value from the second heating run was recorded. For the determination of the T_g of RLZ, it was heated till its melting point and kept for 1 min at the same temperature to ensure complete melting. To the melted RLZ, liquid nitrogen was poured over it to convert it into amorphous form. Its T_g was determined at a heating rate of 20 ^{o}C/min till 140 ^{o}C in DSC.

3.2.5 FT-IR characterization

FT-IR spectra was obtained in the region of 400-4000 cm^{-1} in attenuated reflectance mode (Bruker, Massachusetts, U.S.A) assisted with ZnSe crystal sample holder. Each sample (pure RLZ, physical mixture of drug and polymer and ASDs of RLZ with each of the polymer in 50:50 weight ratio) was placed on the sample holder and scanned between the given range with an average of sixty-four scans and a resolution of 2 cm^{-1} [177] [178].

3.2.6 Solid-state NMR

To study the molecular and structural insight to the drug-polymer interactions, ssNMR experiments were recorded at 298 K using Bruker 750 MHz Avance III spectrometer connected with a variable temperature unit. Topspin 3.6.2 pl6 and Topspin 4.1.3 Bruker NMR software were used for data acquisition and processing. ssNMR experiments were carried out on a 3.2 mm HXY triple resonance probe, and for better sensitivity, it was configured to double resonance mode. 1D ^{13}C cross polarization magic angle spinning (CP-MAS) experiment was recorded with an optimized cross-polarization (CP) contact time of 3 ms at a MAS frequency of 12 kHz. Linear gradient pulse of ramp 100-70 was used during cross-polarization. ^{1}H 90^{o} pulse of 3.3 mS corresponding to a RF of power 76 kHz and ^{13}C power was kept ~ 56 kHz. Proton RF power of 76 kHz was used during acquisition of the decoupling. A total of 1024 scans were acquired for each spectrum with a spectral width of 56818 Hz, corresponding to an acquisition time of 18 ms. Data processing was done using the window function (exponential multiplication) with a line broadening of 50 Hz. The interscan delay was 5 s for all experiments.

3.2.7 Crystallization tendency of amorphous solid dispersion

Thermal analysis of RLZ, polymers and RLZ ASDs prepared with different drug polymer compositions (90:10, 70:30, 50:50, 30:70 and 10:90) were subjected to heat-cool-heat

cycle. The temperature range for the analysis was -20-140 ^{o}C. The starting point of temperature was at 25 ^{o}C. The heating rate was 10 ^{o}C/min [179].

3.2.8 Microscopic analysis

Transmission electron microscopy (TEM) studies were conducted for determining the morphology of drug, ASDs and the state of ASDs after its exposure to 90 ^{o}C for 12 hours. The microscopic analysis was done to detect the possible phase separation on exposure to a higher temperature. The study of phase separation due to moisture exposure was avoided pertaining to its unknown effect on solubilities [148]. The study was done to access the thermodynamic stability of ASDs of RLZ with each of the three polymers. For this analysis, thin ASD films of RLZ with the respective polymers in a 1:1 mixture of DCM and methanol was prepared. 100 µl of solution was spin coated (EZ spinSD, Apex Instruments, India) on a 1cm^2 glass substrate and 200 mesh copper grids to be analyzed under SEM (MA15/18, CARL ZEISS MICROSCOPY LTD) and Tecnai G2T20 LaB6 TEM operating at 200 kV respectively.

3.2.9 Drug polymer miscibility study and phase diagram

3.2.9.1 Melting Point Depression Study

For melting point depression study, 3-5 mg of samples (100% w/w 95% w/w, 90% w/w, 85% w/w and 80% w/w of drug with each polymer) were taken in hermitically sealed aluminum pans and heated under DSC from 20 ^{o}C to 140 ^{o}C at a rate of 2 ^{o}C/min. 50 ml/min nitrogen flow was maintained throughout the DSC run. The readings have been taken in triplicate and mean of the onset of melting point have been reported.

3.2.9.2 True density

The density of the drug and the polymers were determined using a helium pyrometer. Prior to the measurements, the samples were kept over P_2O_5 for 24 hours. The readings were taken in triplicate [180].

3.2.10 Long term stability study

ASDs prepared in the drug:polymer ratio of 50:50 were stored at 25 ^oC 60 % RH. The The long term stability study samples were analyzed at 3, 6, 9, and 12 months. The analysis were done by XRD for the evaluation of any recrystallization over the storage time period.

3.3 Results and Discussion

3.3.1 In silico studies

3.3.1.1 Preparation of 3D structures of polymers

The selection of the most appropriate polymer for preparing an ASD depends upon the interactions between drug and polymer. In order to assess the drug-polymer interactions, accurate or close to accurate 3-dimensional structures of both drug and the polymer are required. Therefore, 3D structures of the three polymers PAA, PVP VA and HPMC AS were modelled initially using computational tools. Modelled polymer chains were subjected to molecular dynamic simulations to obtain the stable conformation of the chains. PAA polymer chain consisting of 20 monomers of acrylic acid acquires a linear geometry (Figure 3.2a, in supporting information). Similarly, PVP VA also exists in linear form containing vinyl acetate and vinyl pyrrolidone linked alternatively (Figure 3.2b). On the other hand, HPMC AS block copolymer acquires a stable bowl shape conformation by forming various intramolecular hydrogen bonds as shown in Figure 3.2c.

The choice of the 20 monomeric units in PAA and PVP VA, and 5 monomeric units in HPMC AS is based on assumption that the optimized structures of the three polymers should possess equivalent surface area and flexibility to interact with RLZ molecule. During molecular dynamics simulation and quantum chemical energy minimization of drug-polymer complexes, the uniformity in the surface area and volume of the complexes can minimize the possibility of inconsistencies. DFT calculation are best performed at the small model system of large polymers to save the calculation time and computational cost, which allow more detailed and precise structural investigations [181,182]. The molar ratio of polymer to drug in the three ASDs in the experimental condition vary for 50%w/w drug load because of the variable molecular weights of the three polymers. For PAA-RLZ ASD, the polymer to drug molar ration is 1923:1, for PVP VA-RLZ ASD, it is 218:1 and for HPMC AS-RLZ ASD, it is 77:1. The DFT calculations of the large polymers collapse because of high degree of freedom and many local minima energy points. When the model system is extended to the actual length, the similar interactions are expected with the other RLZ molecules with the long polymer chains in ASDs.

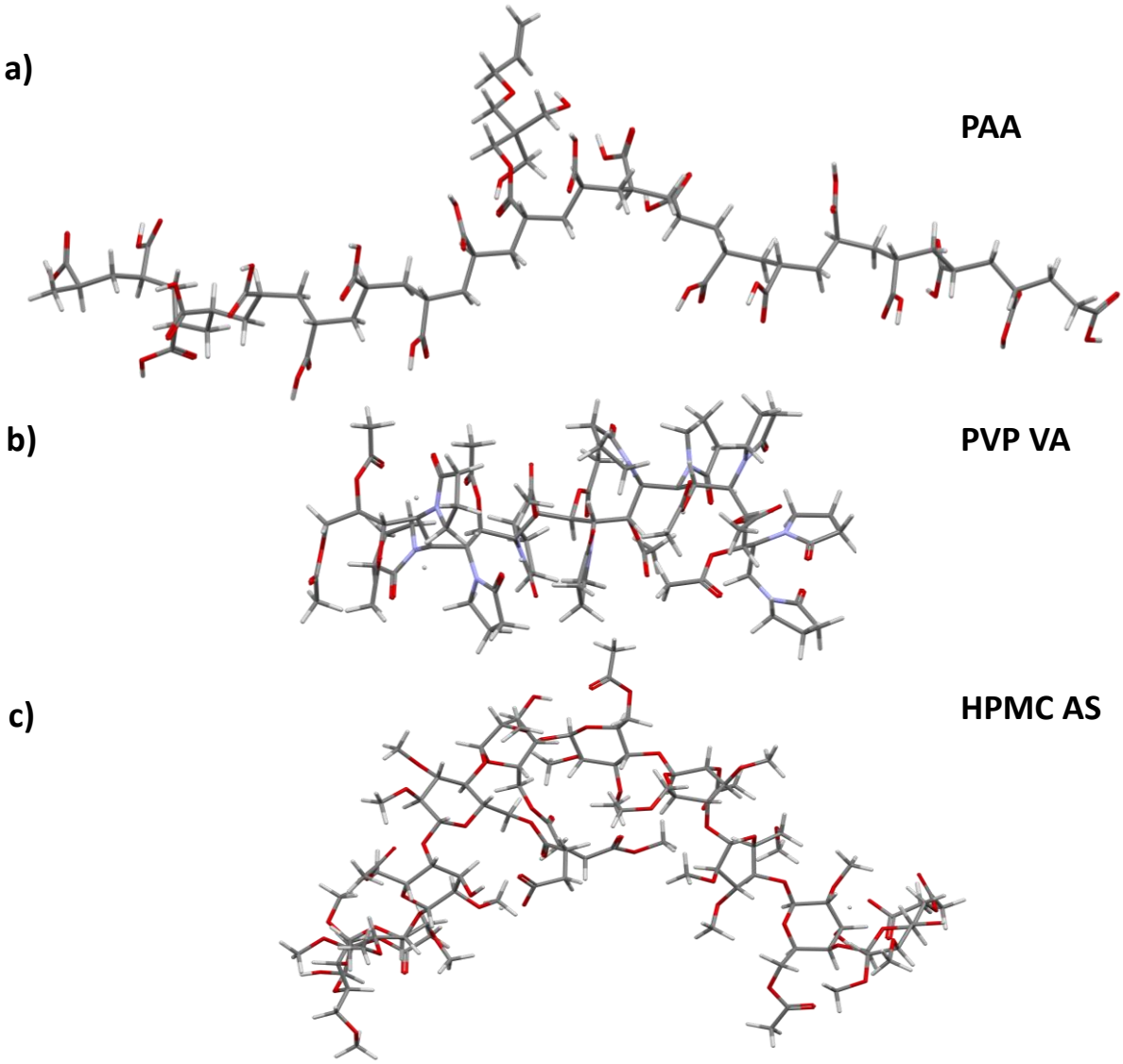

Figure 3.2. Modelled 3D structures of polymers (a) PAA, (b) PVP VA, and (c) HPMC AS

3.3.1.2 Drug-polymer interaction

To determine possible drug-polymer interactions, drug-polymer complexes are obtained in three steps. Firstly, RLZ was docked on the simulated geometries of PAA, PVP VA and HPMC AS at multiple sites around the polymeric chains so as to obtain the initial RLZ-polymer complexes for further quantification of interaction energies. At the second step, the docked complexes were subjected to molecular dynamics simulation to obtain the best fit of drug within the flexible polymer cavity. In the last step, DFT calculations were performed on the simulated complexes to calculate the precise interaction energies

between drug and polymer. In the docking studies, the most stable docked poses resulted the complexes with docking score -4.15, -3.83 and -4.14 kcal/mol for PAA, PVP VA and HPMC AS, respectively. Based on the initial assessment through molecular docking the stability of RLZ-polymer complexes was found to be in the order RLZ-PAA > RLZ-HPMC AS > RLZ-PVP VA. In the three complexes, the free NH_2 group of RLZ shows hydrogens bonding interactions with the oxygen of carboxylic acid or ester groups of the polymers. RLZ resides at the surface of the polymers, however the additional hydrogen bonding interaction is visible between ring nitrogen of RLZ and carboxylic acid group of HPMC AS. The C–H···F and van der Waals interactions in RLZ-PAA lead to increase the docking score higher than that of RLZ-HPMC AS (Figure 3.3). However, the docking scores usually do not take the electron density based interaction into account. Thus, to further validate the order of the stability and quantify the strength of interaction in terms of energy values more robust computational algorithm that is DFT calculations were performed. RLZ, polymers and RLZ-polymer complexes were optimized using ONIOM method, wherein RLZ was optimized using density functionals and polymer segment was optimized using semi-empirical method. The drug-polymer complex formation is an endergonic process for which the interaction energies were calculated in gas phase and in MeOH solvent. The interactions energies for RLZ-PAA, RLZ-PVP VA and RLZ-HPMC AS in gas phase were calculated to be 2.29, 2.64 and 15.24 kcal/mol, respectively. The interaction energies in MeOH solvent were found to be 10.75, 11.37 and 25.06 kcal/mol for RLZ-PAA, RLZ-PVP VA and RLZ-HPMC AS, respectively. Based on the interaction (complexation) energy values, the order of the stability was RLZ-PAA > RLZ-PVP VA > RLZ-HPMC AS under both gas phase and solvent conditions. The normalized interactions energies were calculated with respect to RLZ-PAA as shown in Figure 3.5. Since, ASDs do not contain the solvent molecule, the gas phase energy value can be correlated with

the experimental results. The optimized geometries of the RLZ-PAA complex indicates that RLZ is fitting well inside the polymer cage. The free PAA was transformed from linear conformation to a folded conformation in the RLZ-PAA complex. There are four types of prominent molecular level interaction visible in the RLZ-PAA, (i) a strong hydrogen bond between ring nitrogen of RLZ and COOH group of PAA, (ii) a strong hydrogen bond between NH_2 group of RLZ and COO– group of PAA, (iii) C–H···O interaction between RLZ and COOH, and (iv) C–H···π interaction between CH_2 linker of polymer and π cloud of thiazole ring of RLZ (Figure 3.5a). In case of RLZ-PVP VA, the most prominent interactions are hydrogen bonding interactions of the two hydrogens of NH_2 of RLZ with COO– and pyrrolidone carbonyl oxygen of PVP VA (Figure 3.5b). The strong hydrogen bonding interaction of NH_2, and ring nitrogen of RLZ with carboxylic groups of HPMC AS are visible in RLZ-HPMC AS complex. An additional C–H···O interaction is also visible; (Figure 3.5c). It was observed that major conformational change occurred in PAA as a result of drug-polymer complexation whereas PVP VA does not allow much conformational change due to its rigid structure. The free HPMC AS polymer was already stabilized by forming multiple intramolecular hydrogen bonds and thus does not undergo further conformational changes after complexation with RLZ. This molecular level observation indicates that PAA may be the suitable polymer for forming a stable drug-polymer non-covalently bonded complex, when a slight energy is provided. PVP VA may be the next better polymer of choice. In order to compare the propensity of RLZ to undergo crystallization, an attempt was made to calculate the non-covalent bonding interaction energies between two RLZ molecules through DFT calculation. The interaction energy for RLZ-RLZ was calculated to be -10.18 kcal/mol, which reflect very strong interactions due to bidirectional dual hydrogen-bonding as shown in figure 3.4. However, the crystallization behaviour of drug in 1:1 ratio of drug-polymer and drug-drug

cannot be compared through DFT calculation, because it provides the quantification of intermolecular interactions at smaller model systems. The interaction energy of -10.18 kcal/mol justifies the requirement of heating (enthalpy) to break these drug-drug intermolecular interactions within the crystal lattice of drug.

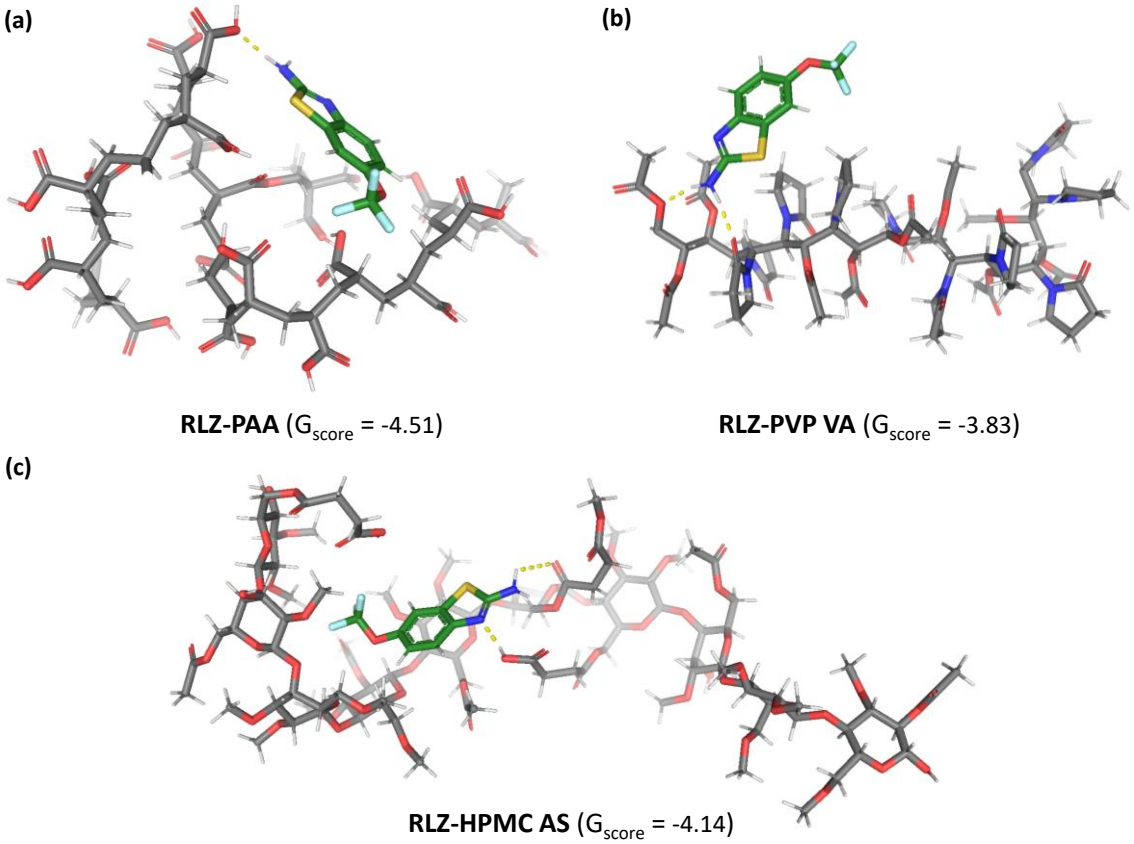

Figure 3.3. RLZ-polymer complexes obtained after molecular docking analysis

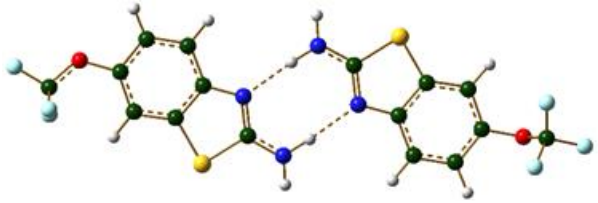

Figure 3.4. Optimized structure of RLZ-RLZ dimeric complex obtained from crystal data

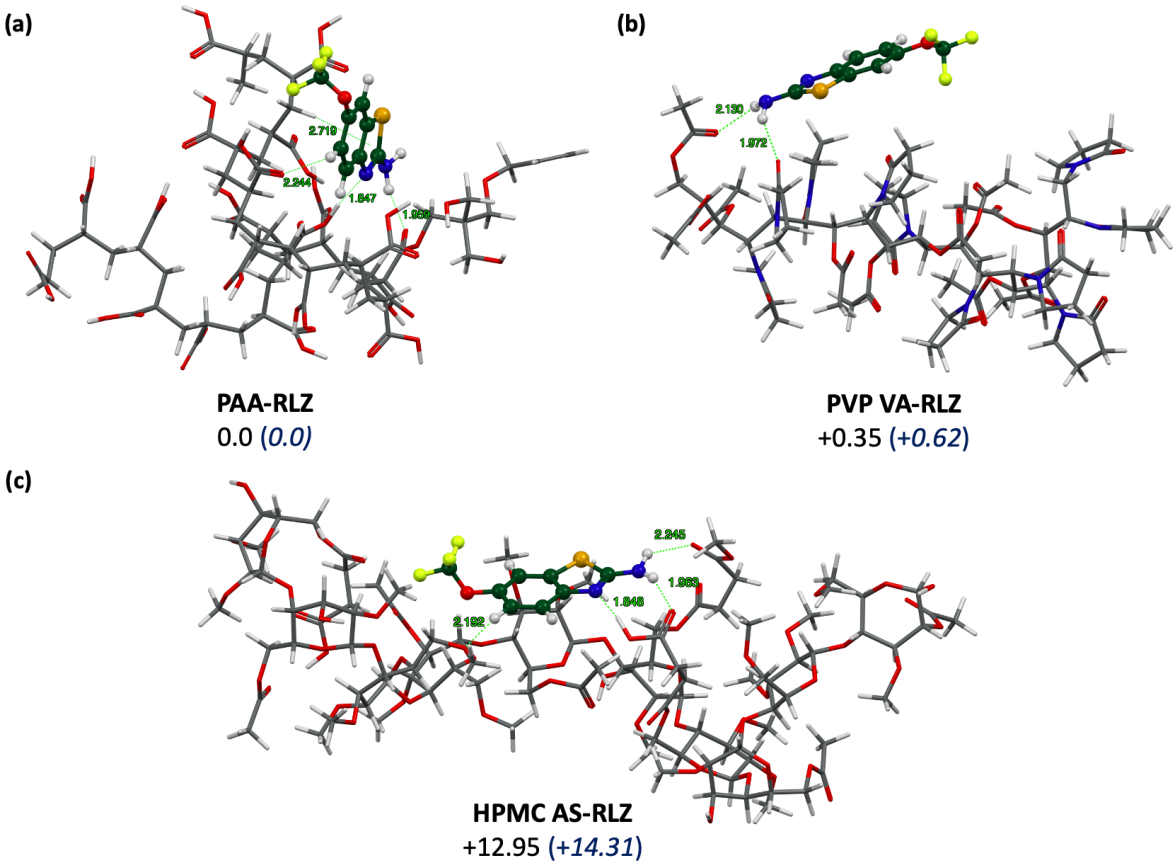

Figure 3.5. RLZ-polymer complexes along with their respective interaction energies. Bond distances are in Å, interaction energies are in kcal/mol. Energy values are the complexation energy values referenced to PAA-RLZ in italics and in brackets are obtained under implicit solvent condition using methanol as a solvent

Docking and MD simulation studies depend upon molecular mechanics wavefunction which is suitable for computational studies of large systems like polymer, lipids and nanocarriers etc. These studies can provide the qualitative determination of molecular behavioral patterns in the simulated conditions. On the other hand, DFT studies depend upon ab initio or semi empirical wavefunctions which are more robust and provide more accurate estimation of energy values. However, DFT studies can be performed on truncated model systems within the agreeable time frame and available computational facilities. DFT studies are more suitable when quantitative comparison and more precise atomic details of molecular interactions are required such as bond distance and bond angle for the interactions. On one hand, simulation of larger system corresponds to the more realistic systems with diverse chemical behaviour, while on the other hand, the smaller

systems lead to quick, more accurate calculations and atomic details but limits the study due to a gap between simulated and realistic systems. The selection of computational methods depends upon the formulation scientist. For example, MD simulation techniques are more suitable when one wants to calculate the physicochemical properties like miscibility, solubility or glass transition temperature of ASDs. DFT calculations are preferred choice when estimation of molecular level interactions, energy calculations or polymer profiling is desired.

3.3.2 Powder X-ray diffraction study

The PXRD pattern of pure crystalline RLZ shows distinct sharp peaks at 9.14^o, 13.64^o, 18.18^o, 22.74^o, and 25.22^o, which indicates the crystalline nature of the drug (Figure 3.6). The PXRD patterns of ASDs with different drug loading (50, 70, and 90 %w/w) with PAA, PVP VA, and HPMC AS show the transformation of the sharp peaks to the absolute halo patterns at 50% w/w drug loading, which indicate the presence of single-phase binary amorphous system. At 70% w/w, a few indistinct sharp peaks can be observed at 19.68^o, and 25.3^o in the case of ASD RLZ-HPMC AS. In ASD RLZ-PVP VA (70:30) also minor sharpness at 19.68^o was observed. After increasing the drug loading to 90% w/w, crystallinity was observed with all three polymers in the order PAA<PVP VA<HPMC AS. Shift in the two theta values RLZ from 18.18^o to ~19.4^o and 25.22^o to 26.6^o could be attributed to the occurrence of polycrystallinity in RLZ after association with the polymer [183]. This is an indication of the presence of two phases in the analyzed ASD. This concludes that the ASD formation capacity of polymers with RLZ is in the order of PAA>PVP VA>HPMC AS.

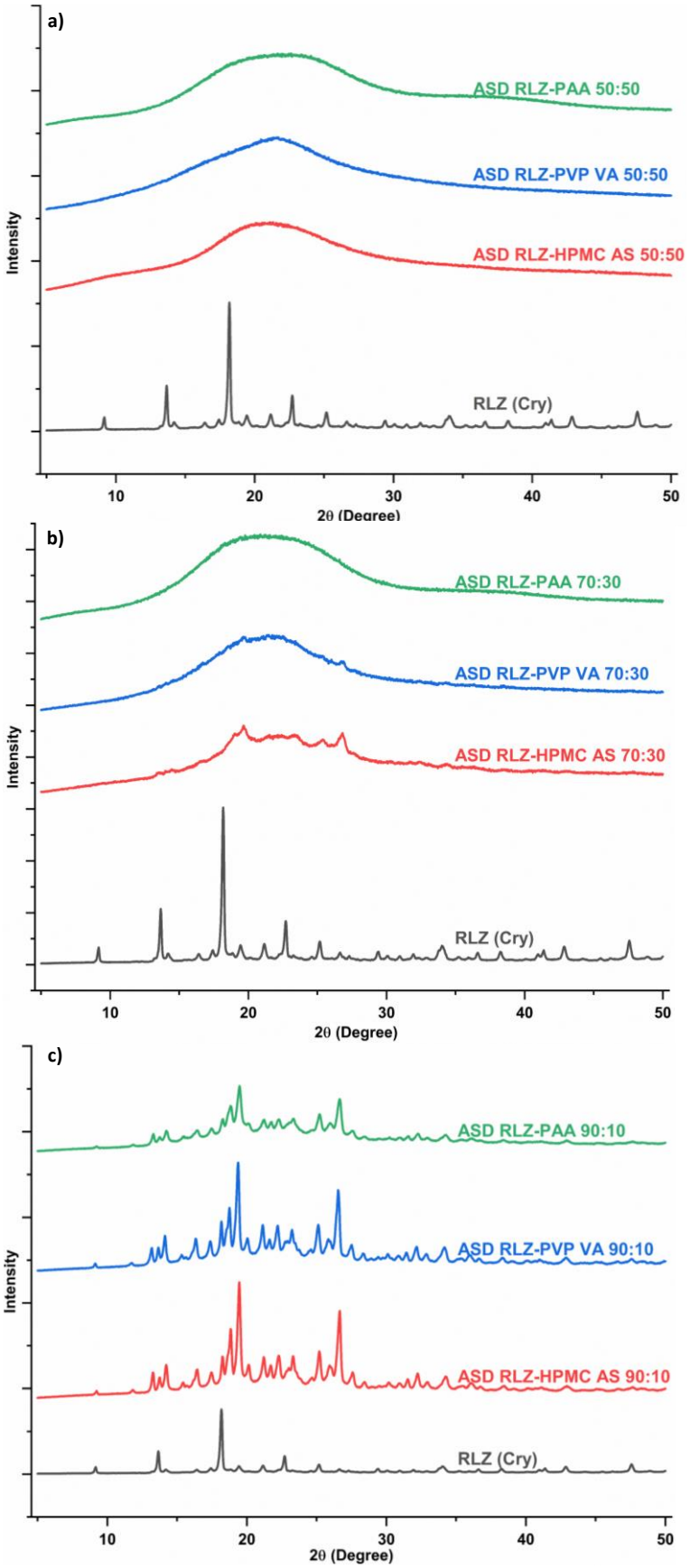

Figure 3.6. Overlay spectra of PXRD patterns of ASDs having (a) 50:50 of RLZ with polymers, b) 70:30 of RLZ with polymer, and c) 90:10 of RLZ with polymer

3.3.3 Determination of melting point and glass transition temperature

T_g is the indicator of molecular mobility, where lower molecular mobility refers to high physical stability of the amorphous systems. DSC is well known for its evaluation of transition process occurring in amorphous solid at a higher temperature at which the surrounding molecules influences the orientation and reorientation of the molecules [184].

T_m and T_g of RLZ, physical mixtures of RLZ with each polymer, and ASDs are shown in Figure 3.7. A melting endotherm was shown by RLZ at 120 ^oC demonstrating its pure crystalline nature, while amorphous RLZ showed a T_g at 28 ^oC (Figure 3.8). When 90:10 ratio of drug-polymer were subjected to heat-cool-heat cycle in the DSC for *in situ* ASD preparation, and the determination of their T_g, sharp endotherm was observed with all the three polymers. This confirmed the absence of *in situ* ASD formation at 10% w/w ratio. At 70:30 ratio of the drug-polymer, the T_g of RLZ-PAA and RLZ-PVP VA were observed at 91 ^oC and 39 ^oC, respectively. However, RLZ-HPMC AS did not show any change in the specific heat capacity and, a melting endotherm was observed confirming that HPMC AS was not efficient to form ASD with RLZ at this weight ratio as well. At 50:50 ratio of drug-polymer, with all three polymers glass transition temperatures were observed. A T_g of 106 ^oC, 53 ^oC, and 40 ^oC were observed for RLZ-PAA, RLZ-PVP VA, and RLZ-HPMC AS, respectively. In the aforementioned cases, a single T_g was observed whenever *in situ* ASD formation occurred inside the DSC. This clearly indicates the formation of a miscible system since the obtained T_g of *in situ* formed ASDs were between the T_g of pure amorphous drug and polymer (Table 2) [185]. This study implies that PAA is imparting most promising stability to the amorphous RLZ followed by PVP VA and HPMC AS.

Table 3.2. T_g of different solid forms of RLZ and ASD with different drug polymer compositions

S.No	Drug to polymer weight ratio	Composition	T_g (°C)
1		RLZ-PAA	106
2	50:50	RLZ-PVP VA	53
3		RLZ-HPMC AS	40
4		RLZ-PAA	91
5	70:30	RLZ-PVP VA	39
6		RLZ-HPMC AS	-
7		RLZ-PAA	-
8	90:10	RLZ-PVP VA	-
9		RLZ-HPMC AS	-
10[a]	NA	PAA	102
11[b]	NA	PVP VA	101
12[c]	NA	HPMC AS	117
13	NA	RLZ (Amorphous)	28

[a] Ref [186], [b]Ref [148], [c]Ref [187]

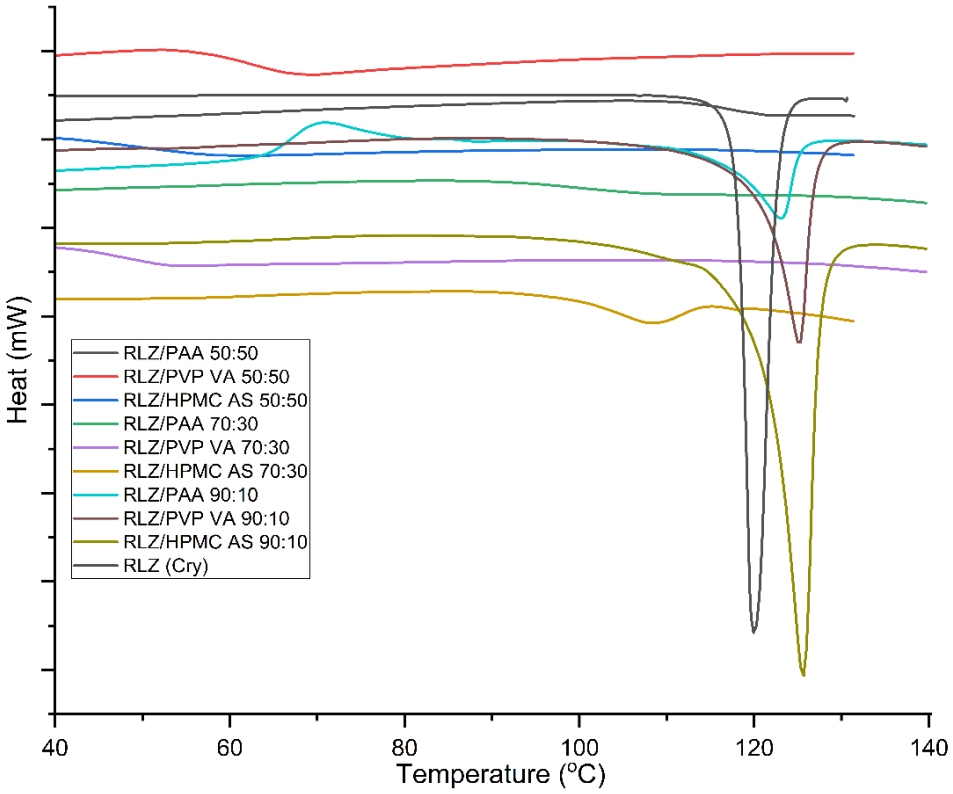

Figure 3.7. Overlay of DSC plots of in situ ASDs of RLZ with each of the polymer in different drug to polymer weight ratios formed inside the DSC with heat-cool-heat cycle

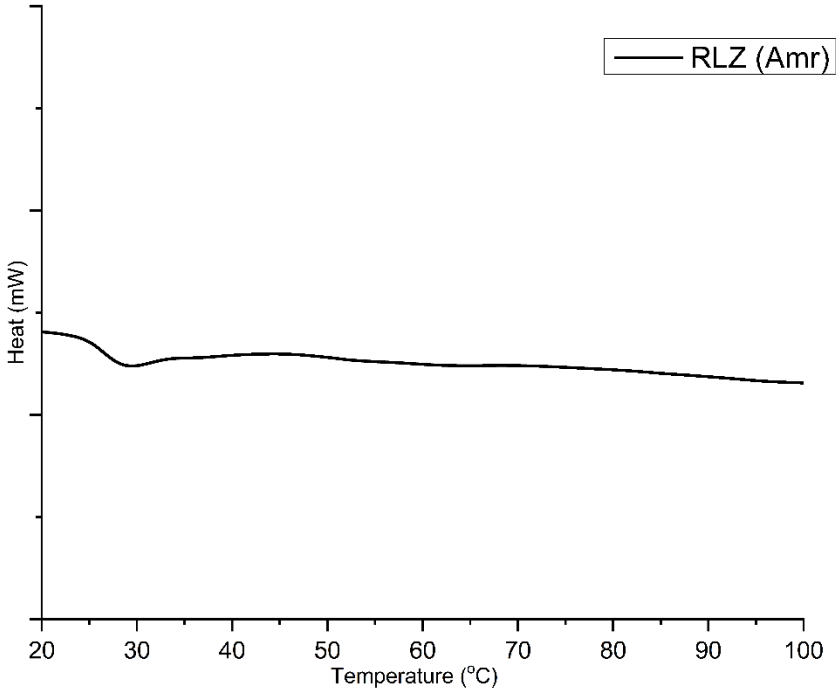

Figure 3.8. Glass transition temperature of amorphous pure RLZ

3.3.4 FT-IR characterization

Figure 3.9 represents the comparative FTIR spectra of RLZ, PMs, and ASDs of RLZ-polymer at a 50:50 weight ratio. In the spectra of RLZ the prominent peaks at 3364 cm^{-1}, 1543 cm^{-1}, 1458 cm^{-1},1293 cm^{-1} and 1143 cm^{-1} correspond to N-H stretching, C=C stretching, C-F stretching, C-O stretching, and C-N stretching, respectively. Comparing the spectra of RLZ with the physical mixture of each polymer, minor differences like the shift from 3364 cm^{-1} to 3368 cm^{-1}, 1538 cm^{-1} to 1543 cm^{-1}, 1293 cm^{-1} to 1300 cm^{-1} and 1143 cm^{-1} to 1203 cm^{-1} were observed in PM RLZ-PAA. In PM RLZ-PVP VA, peaks were observed at 3366 cm^{-1} and 1541 cm^{-1}. In PM RLZ-HPMC AS, the characteristic peaks were observed at 3323 cm^{-1}, 1248 cm^{-1}, and 1213 cm^{-1}. However, in the case of ASDs, much more changes in the wavenumber were observed. The N-H stretching peaks were broadened significantly in the ASDs. The C=C stretching peaks were shifted to 1528 cm^{-1} (in ASD RLZ-PAA) and 1538 cm^{-1} (in ASD RLZ-PVP VA and ASD RLZ-HPMC AS). The C-O stretching, C-N stretching and C-F stretching peaks were also shifted in the

ASD samples. These shifts in wavenumber confirmed the formation of ASD and presence of interactions between drug and polymer. The evidence of strong drug-polymer interactions assures the formation of a highly stable ASD by increasing the onset temperature of crystallization and by attenuating the crystallization of the drug [188].

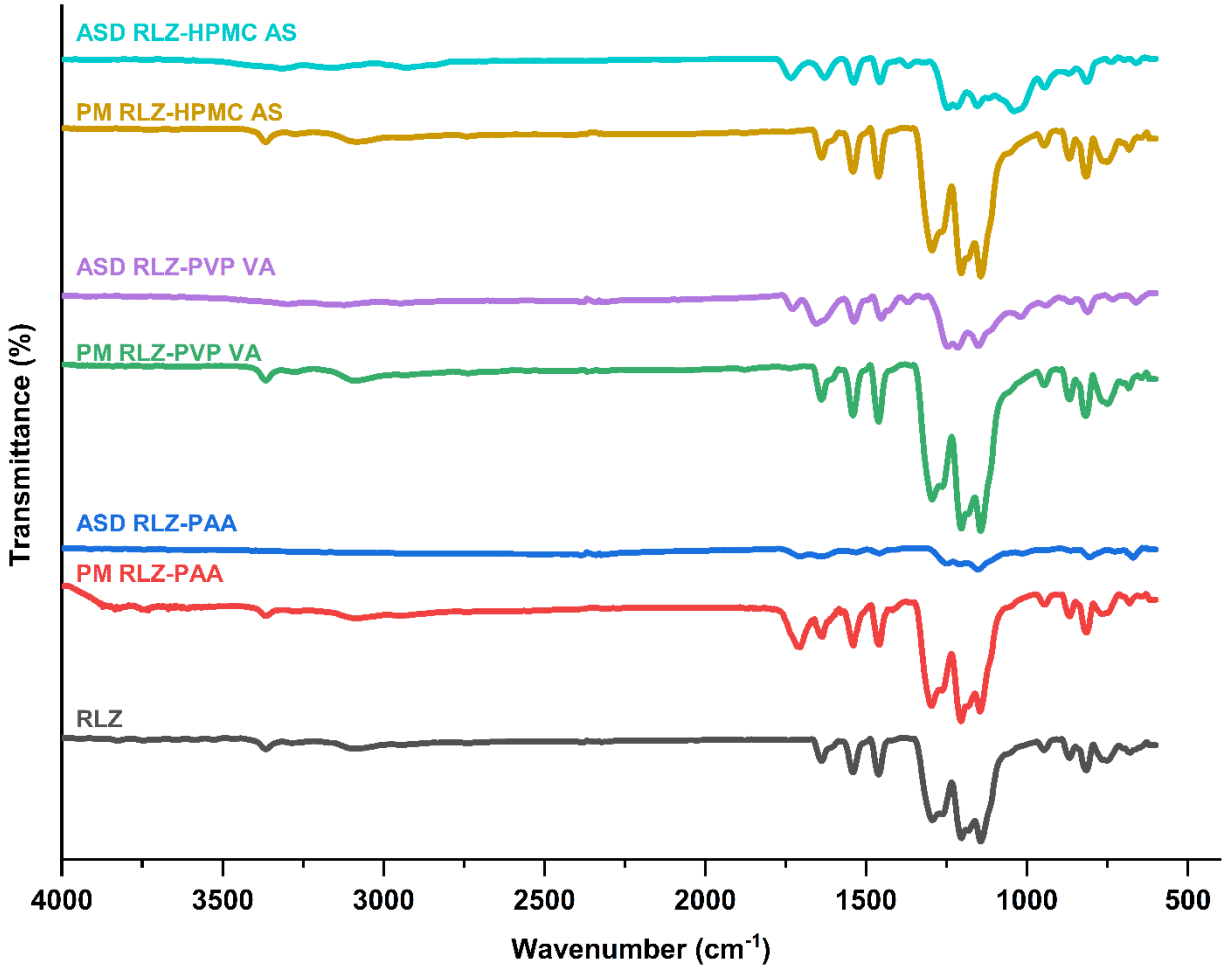

Figure 3.9. FTIR spectra of RLZ, physical mixture of RLZ with polymers and ASD of RLZ with each of the respective polymer

3.3.5 Solid-state NMR

ssNMR is a very powerful tool to identify the presence of molecular interactions between the drug and the polymer, responsible for the stability of ASD. The ^{13}C CPMAS spectra of crystalline RLZ, pure polymers, and RLZ ASD with each of the polymers in the ratio of 70:30 were recorded to study the interactions occurring at the molecular level. The typical sharp resonances in the spectra of pure RLZ are reflecting the crystalline nature

of RLZ. In the spectra of ASDs, the peaks of both drug and polymer are merged hence confirming the formation of molecular level dispersion. The broad Gaussian resonances are indicative of disorder in the crystal arrangement as seen in amorphous solid [42]. ASD RLZ-PAA is showing more nonhomogeneous line broadening with respect to ASDs RLZ-PVP VA and RLZ-HPMC AS, which could be possible due to more random distribution of the chemical environment subjected to more loss of crystallinity [189] in comparison to the former and the presence of a small amount of crystalline drug in the later two spectra. This is also in close agreement with the results obtained in PXRD studies and *in silico* studies.

The overlay of pure RLZ and ASD RLZ-PAA ^{13}C CP/MAS spectra shows the downfield shift in the quaternary carbon (C_a) of the thiazole ring from 169 to 170 ppm, as shown in Figure 3.10a. Another quaternary carbons (C_e and C_c) of pure RLZ occurring at 150 and 143 ppm, respectively, are getting merged with the C_b in the case of ASD RLZ-PAA. A similar observation is found for another aromatic carbon C_h and C_g, which are occurring at 132 and 129 ppm, respectively. The trifluoromethyl carbon (C_f) shown at 120 ppm is also merged with the aromatic C_d carbon of RLZ. The downfield shift from 178 ppm to 180 ppm in the carbonyl carbon ($C_{a'}$) and from 37 ppm to 43 ppm in the methylene carbon ($C_{b'}$) of PAA [190] indicate that these carbons are experiencing the electron-withdrawing effect through non-covalent interactions. The merging of peaks and changes in the ^{13}C chemical shifts explain the rigidity in the structure due to the prominent interaction between RLZ and PAA functional groups.

In the case of PVP VA (Figure 3.10b), the resonance at 175 and 168 ppm are assigned to the carbonyl carbons of the pyrrolidone ($C_{a'}$) and acetate ($C_{i'}$) functionality, respectively. Resonances of 65 and 34, 18 and 16 ppm are assigned to $C_{g'}$, $C_{f'}$, $C_{c'}$ and $C_{j'}$ carbon respectively. However, the carbon present in the pyrrolidone ring ($C_{b'}$) and the vinyl chain

($C_{h'}$) have been assigned resonance values of 40 and 29, respectively [146]. Despite the ASD RLZ-PVP VA showing evidence of the formation of the molecular dispersion, there is clearly the presence of crystalline RLZ which is evident by the sharp resonances. The interaction could be seen in the shortening and the slight deshielding of the carbons present in the range of 40-15 ppm of PVP VA. Hence, it can be inferred that despite of interaction shown by the polymer the crystalline structure of RLZ persists making it a two-phased dispersion. In Figure 3.10c, the anomeric carbons labeled as a', d', b', c', and e', j' are responsible for resonances lying between 101-58 ppm for polymer HPMC AS. At 67 and 56 ppm there are shoulders due to methylene $C_{f'}$, and methoxy carbons ($C_{i'}$ and $C_{h'}$), respectively. The most shielded carbons lying in the range of 26-14 ppm are those in the acetyl ($C_{h'}$), succinoyl chain ($C_{n'}$ and $C_{o'}$) and methyl carbon ($C_{l'}$) in the hydroxypropyl chain. Interactions between RLZ and polymer in ASD RLZ-HPMC AS can be seen through the deshielding of carbons lying between 100-58 ppm of HPMC AS, but the resonances of RLZ seem unaffected in terms of chemical shifts; however, there is a change in the peak intensities from that of the crystalline RLZ.

Hence, it can be concluded that the interaction and the capacity to make a stable amorphous solid dispersion system by the polymer is in the order of PAA > PVP VA > HPMC AS. These results corroborate the findings from the *in silico* work.

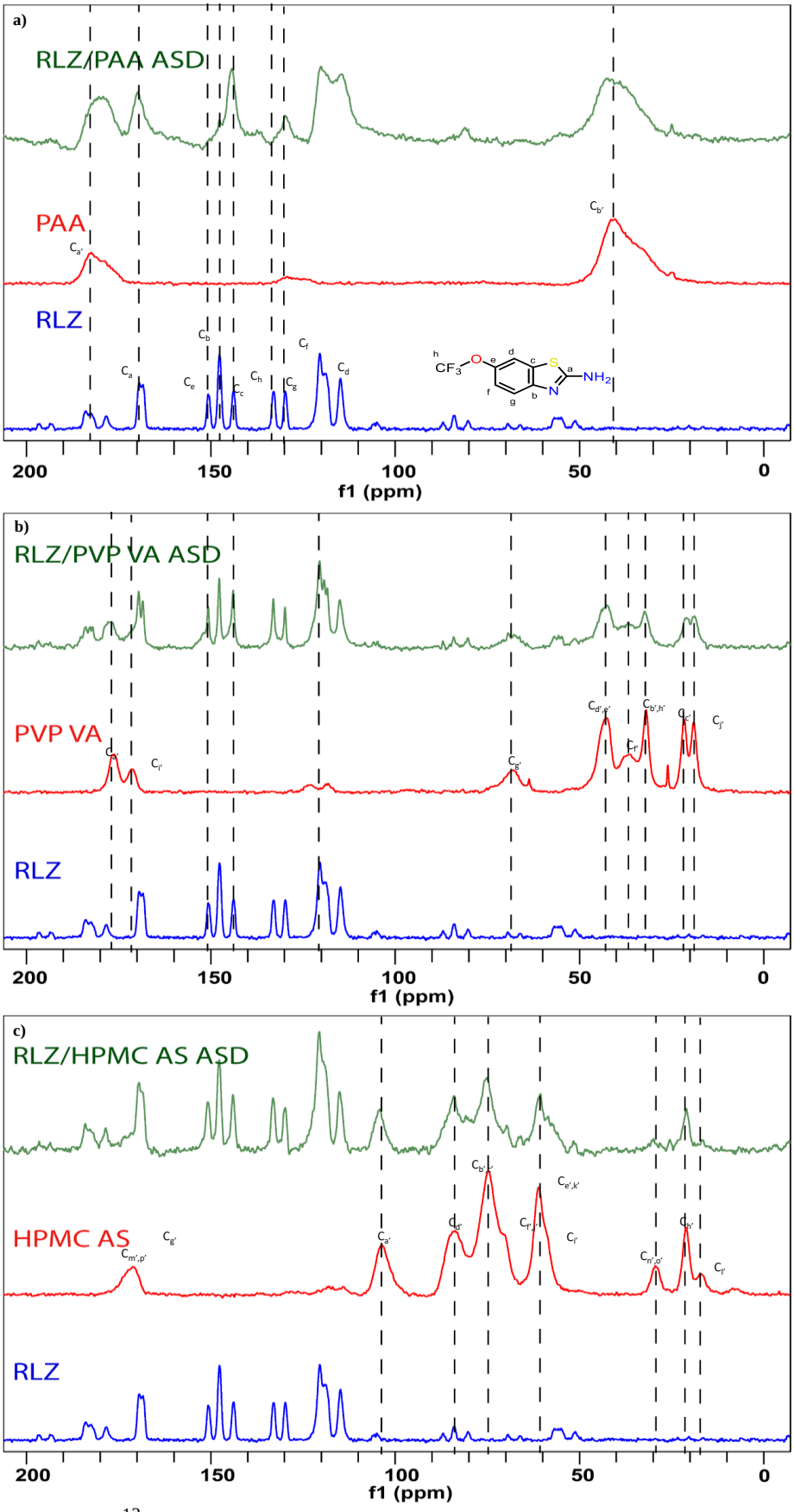

Figure 3.10. The ^{13}C CP-MAS spectra of RLZ in comparison with a) PAA and ASD RLZ-PAA, b) PVP VA and ASD RLZ-PVP VA, and c) HPMC AS and RLZ-HPMC AS

3.3.6 Crystallization tendency of amorphous solid dispersion

Heat-cool-heat cycle in DSC was used to assess the crystallization tendency of drug in the prepared ASDs. The thermograms of RLZ ASDs prepared with different composition of drug and polymer are shown in Figure 3.11 a, b, and c. Fusion and crystallization enthalpies of RLZ and RLZ ASDs are mentioned in table 3. In the thermograms it can be seen that the samples with higher weight percentage of drug (90% w/w) the cooling crystallization event is prominent in ASDs prepared with all the polymers. The enthalpy of fusion values are in close agreement with the enthalpy of crystallization values showing the extent of crystallization occurring in 90% w/w drug loaded ASDs. Exothermic effect due to the crystallization of RLZ were not observed in the ASDs prepared with polymer wight percentage of 30% to 90%. A slight event of crystallization was observed in RLZ ASDs prepared HPMC AS at 70% w/w drug loading. The crystallinity estimated from the fusion of enthalpy were around 15%, 16% and 29% for 90:10 RLZ-PAA, RLZ-PVP VA, and RLZ-HPMC AS ASDs respectively. This gives an indication that solid dispersions of RLZ when prepared with PAA and PVP VA will offer highest resistance against drug recrystallization followed by ASD prepared with HPMC AS. The higher value of crystallinity describes the higher mobility of HPMC AS [179]. This confirms the higher kinetic stability of ASDs prepared with PAA and PVP VA with respect to HPMC AS.

Table 3.3. Fusion enthalpies (ΔHm) and crystallization enthalpies (ΔHcr), with corresponding onset temperatures of RLZ and its ASDs with polymers in different compositions

Enthalpy	**ΔH_{cr} (Jg^{-1})**					**ΔH_m (Jg^{-1})**				
RLZ	-332.94 (87.25 °C)					341.82 (119.36 °C)				
ASDs	90:10	70:30	50:50	30:70	10:90	90:10	70:30	50:50	30:70	10:90
RLZ: PAA	-49.94	-	-	-	-	52.87	-	-	-	-
RLZ: PVP VA	-51.65	-	-	-	-	55.57	-	-	-	-
RLZ: HPMC AS	-95.18	-23.88	-	-	-	101.73	-	-	-	-

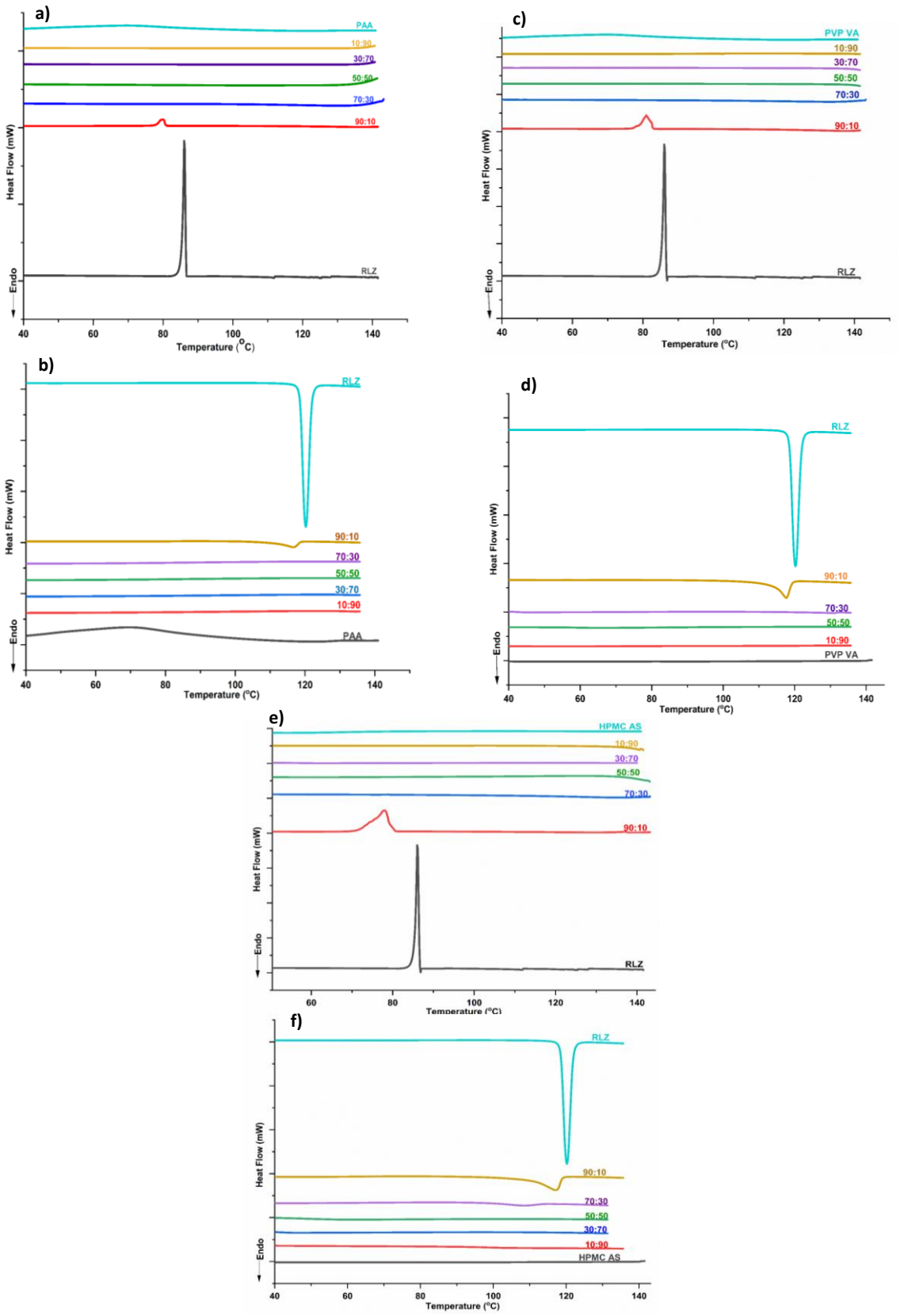

Figure 3.11. DSC curves of RLZ ASDs of different compositions with PAA, PVP VA and HPMC AS a), c) and e) represent cooling and b), d) and f) represent second heating in the heat-cool-heat cycle

3.3.7 Microscopic analysis

The TEM images of ASDs have been taken in pre- and post-annealed conditions. TEM with the selected area electron diffraction (SAED) patterns was used to identify the regions where crystallinity might have developed due to annealing. Figure 3.12 shows the bright field images of the ASDs for the pre- and post-annealed conditions. A large sample size (50 areas on each grid) was chosen to study the morphology of RLZ ASDs. The bright field TEM images (Figure 3.12 (a, e and i)) show the spherical morphology of ASDs prepared with the polymers. The diffused rings produced by the particles in the SAED pattern confirm their amorphous nature [191]. The TEM images of all three ASDs were observed for the post-annealed condition and found that no significant change has occurred in RLZ-PAA ASD (Figure 3.12). However, in the RLZ-PVP VA and RLZ-HPMC AS ASD, the bright field images along with SAED showed a high degree of crystallization as there was the presence of a regular array of diffraction spots (Figure 3.12 (g,h) and (k,l)) [122,124]. The SAED pattern consists of systematic spots which means the grains or crystallites formed are in the ranges of nm length scale. Along with the array of diffraction, diffused circular rings can also be seen in the pattern explaining the presence of both amorphous and crystalline regions. To confirm the presence of RLZ only, the crystallographic information was collected from the CIF file [192] and it showed that the compound belongs to the triclinic system with a space group of $P\bar{1}$ suggesting that the crystal has got center of inversion (centrosymmetric). As per the crystallography data available on the Cambridge Crystallographic Data Centre (CCDC), the lattice parameters of RLZ are: a=8.08 Å, b= 11.78 Å, c=19.74 Å and $\alpha = 78.44^{o}$, $\beta = 84.378^{o}$, $\gamma = 89.318^{o}$. The information obtained from the zone axis table of Figure 3.12 h and l indicated that the crystals present have the zone axis of [311] and [-112] which corresponds to the RLZ crystals.

The presence of RLZ crystals due to demixing after annealing from the supersaturated ASD is in agreement with the T_g results. It appears that due to high T_g, ASD RLZ-PAA exhibited superior stability in comparison to RLZ-PVP VA and RLZ-HPMC AS ASD and retained its amorphous form at higher temperatures. This confirms the suitability of PAA as polymer over PVP VA and HPMC AS for the preparation of a thermodynamically stable ASD with RLZ. The chemical stability of all the three ASDs of RLZ with PAA, PVP VA and HPMC AS, which were estimated through HPLC, was in line with the thermodynamic and kinetic stability. This may also confirm that after demixing the recrystallized component was RLZ only.

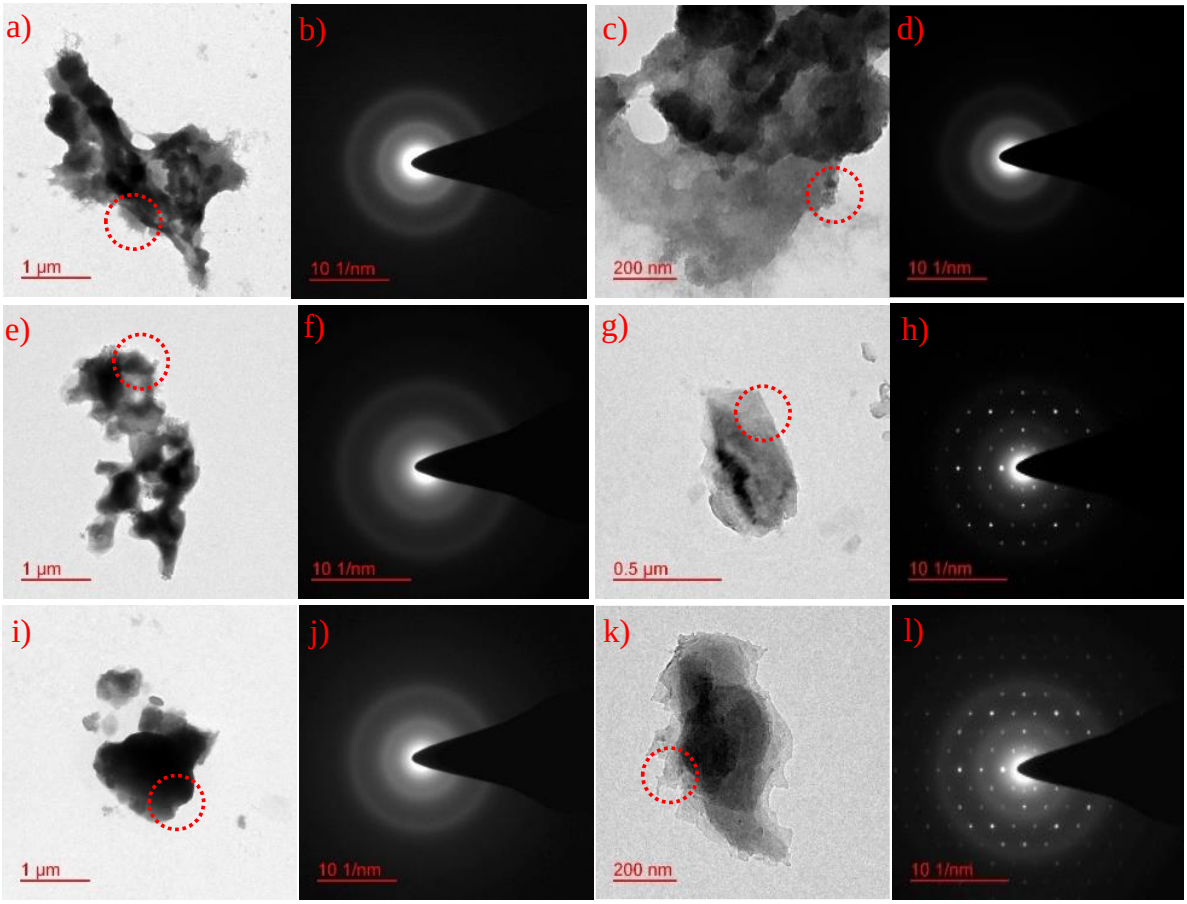

Figure 3.12. Bright-field images of (a) freshly prepared RLZ-PAA ASD, (c) annealed at 90°C for 12 hrs RLZ-PAA ASD, (e) freshly prepared RLZ-PVP VA ASD, (g) annealed at 90°C for 12 hrs RLZ-PVP VA ASD, (i) freshly prepared RLZ-HPMC AS ASD, (k) annealed at 90°C for 12 hours

3.3.8 Drug polymer miscibility and phase diagram

The determination of miscibility of drug in polymer is widely estimated by Flory-Huggins theory. This theory explains the thermodynamics of the mixing of polymers with solvent molecules by using the Flory-Huggins interaction parameter χ [193]. The degree and type of interaction play a major role in free energy of mixing (ΔG_{mix}), which can be determined by equation 3.1.

$$\frac{\Delta G_{mix}}{RT} = \Phi_{drug} ln \Phi_{drug} + \frac{\Phi_{poly}}{m} ln \Phi_{poly} + \chi \Phi_{drug} \Phi_{poly} \qquad \text{Equation 3.1}$$

Where Φ is the volume fraction of the drug and the polymer; R is the universal gas constant; T is the absolute temperature of the system; m is the ratio of the volume of a polymer chain to drug molecular volume [194,195]. Equation 3.1 shows the contribution of the entropy and enthalpy of mixing of drug and polymer, which are represented by the first and second terms, respectively. Entropy is the decisive factor in the determination of spontaneous mixing since enthalpy always favours the mixing. It is so because the enthalpy of mixing cannot surpass a small critical value unless any phase separation occurs.

To determine the entropy of mixing the two components, interaction parameter (χ) (shown in equation 3.2) was calculated by the melting point depression method, which is an indicator of the decreased chemical potential of drug in the mixture with respect to the pure crystalline drug [51].

$$\frac{1}{T_m} - \frac{1}{T_m^o} = -\frac{R}{\Delta H_f}\left[\ln \Phi_{drug} + \left(1 - \frac{1}{m}\right) \Phi_{poly} + \chi \Phi_{poly}^2\right] \qquad \text{Equation 3.2}$$

Where T_m is the drug's melting temperature in the mixture of drug and polymer, T_m^o is the melting point of the pure crystalline drug, Φ is the volume fraction of the drug and polymer and ΔH_f is the heat of fusion of the pure crystalline drug. The DSC plots shown

in Figure 3.13 indicate the depression in the onset of the melting point of RLZ with varying weight fractions (Φ_{poly}) of each polymer. Figure 3.13 shows that increase in weight fraction of each polymer is proportionately related to the depression in the onset of melting point of the crystalline RLZ. This verifies that there is a certain degree of mixing between the drug and polymer near the melting temperature of the drug in the respective compositions of physical mixtures. Using equation 3.2 (values of the required parameters are mentioned in Table 3.4), χ of drug with each of the polymers were calculated. The calculated χ were plotted against temperature empirically described by equation 3.3 to show its dependence on temperature.

$$\chi = A + B/T \qquad \text{Equation 3.3}$$

Where A and B/T are the relative contributions of entropy (temperature-independent) and the enthalpy, respectively towards the free energy of mixing. T is the melting temperature of drug in a drug-polymer mixture. Equation 3.3 is a representation of straight-line equation, where the value of R^2 were 0.9477, 0.9817, and 0.9410, respectively, for physical mixtures of RLZ-PAA, RLZ-PVP VA, and RLZ-HPMC AS showing the goodness of fit in χ vs 1/T plot (shown in Figure 3.14). Hence, by using the value of A and B, the value of χ was extrapolated for even lower temperatures.

Table 3.4. Physical properties of RLZ, PAA, PVP VA and HPMC AS used for quantitative drug-polymer miscibility

S.No.	Components	Molecular weight (g/mol)	True Density (g/cm^3)	Molar volume (cm^3/mol)	ΔH_f (kJ/mol)	T_m (K)
1	RLZ	234	1.66	140.96	18043.74	391.98
2	PAA	450000	1.33	338345.86	-	-
3	PVP VA	51000	1.13	45132.74	-	-
4	HPMC AS	18000	1.23	14634.15	-	-

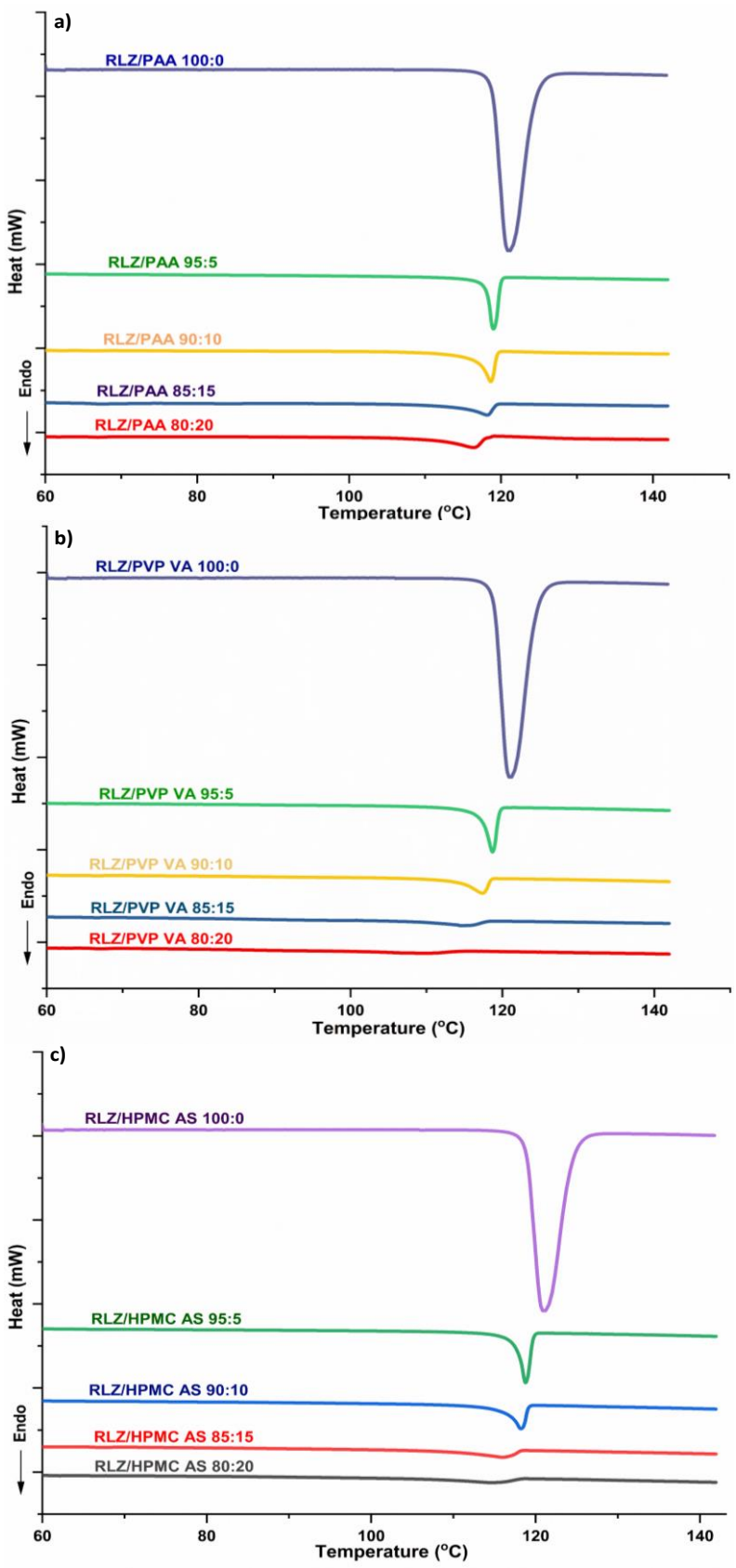

Figure 3.13. DSC plots of depression in melting point onset of drug- a) PAA b) PVP VA and c) HPMC AS physical mixture at a heating rate of 2°C/min.

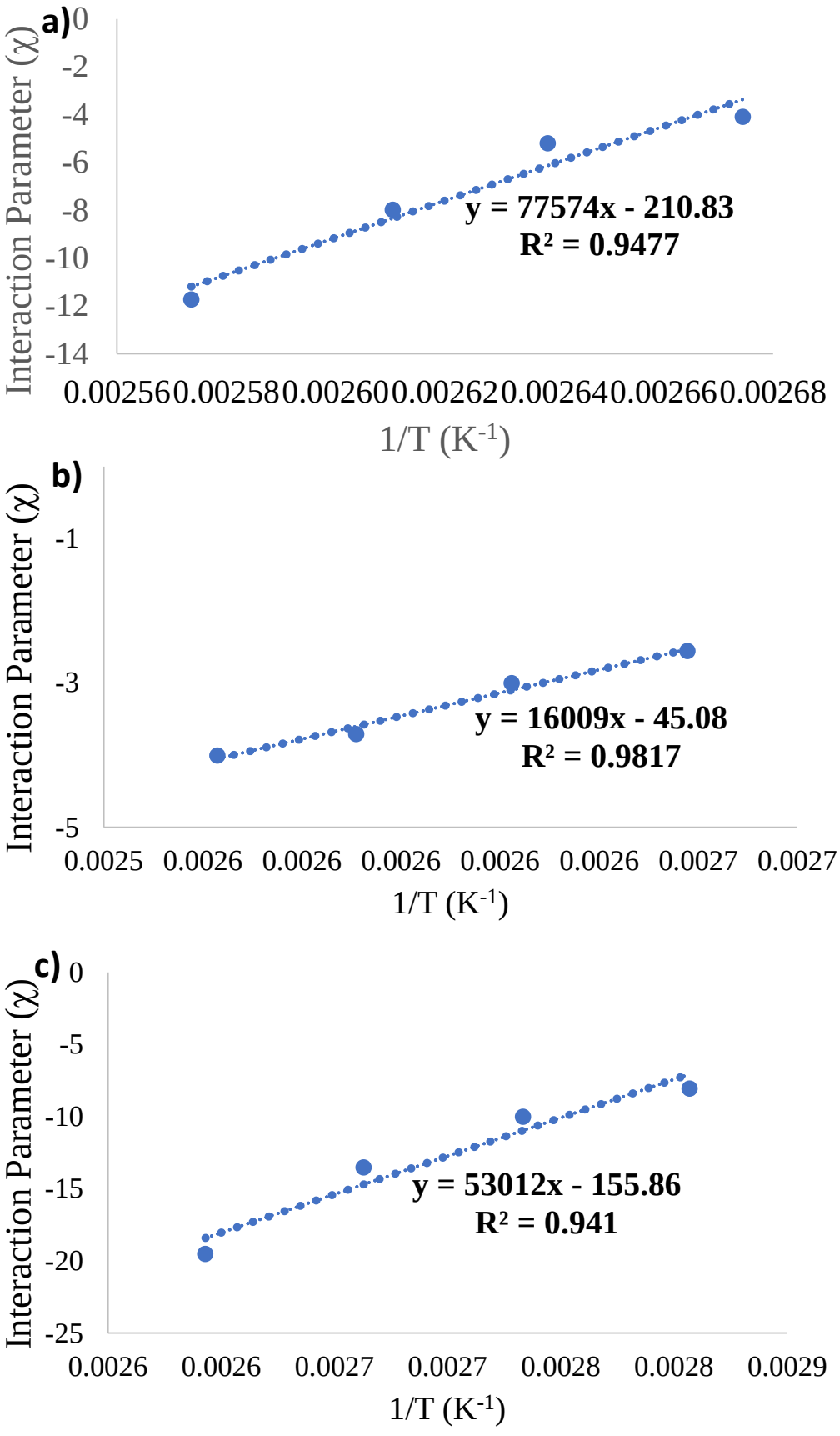

Figure 3.14. F-H interaction plot of the physical mixtures of drugs and polymers with respect to temperature

In the case of drug-polymer miscibility, since the miscible diluent is a polymer that, which is amorphous in nature, the entropy of mixing becomes negligible [196]. Hence, the second derivative of the free energy (equation 3.1) is equated to zero and as stated in equation 3.4, the maximum drug-polymer miscibility boundary may be calculated as:

$$T_S = \frac{2B}{\left(\frac{1}{\Phi_{drug}}\right)+\left(\frac{1}{m\left(1-\Phi_{drug}\right)}-2A\right)}$$ Equation 3.4.

Drug solubility and miscibility can be plotted as a function of drug weight fraction and temperature after the understanding of how ΔG_{mix} varies as a function of T for each system.

ΔG_{mix} is an indicator of a stable drug-polymer system and was calculated using χ through equation 3.1 and then $\Delta G_{mix}/RT$ was plotted against the drug volume fraction (Φ_{drug}). The negative value of ΔG_{mix} in all the three systems was seen across all drug weight fraction near the melting point of the drug. This shows the thermodynamic stability of all three drug-polymer systems near drug's melting point. $\Delta G_{mix}/RT$ vs Φ_{drug} were also plotted at T_g shown by each drug-polymer system prepared by *in-situ* ASD formation inside DSC instrument (discussed in previous section). In this curve shown in Figure 15 a, b, and c it was seen that all the drug-polymer system at 106^{o}C (T_g of 50:50 RLZ-PAA ASD), ΔG_{mix} is negative and convex across all Φ_{drug}. However, at 53 ^{o}C (T_g of RLZ-PVP VA ASD) and at 40 ^{o}C (T_g of 50:50 RLZ-HPMC AS ASD), all the systems showed instability due to positive ΔG_{mix} at their respective T_g, which may result into heterogeneous drug-polymer mixture. It is noteworthy that RLZ-PAA showed negative ΔG_{mix} at its T_g while RLZ-PVP VA and RLZ-HPMC AS showed positive ΔG_{mix}. Contrary to this result, in experimental settings, we observed single T_g of freshly prepared ASDs, which correspond to the single phased drug-polymer system. Usually, immiscible-systems, two different glass transition temperatures are observed, one for drug and another for polymer [197].

Miscibility study is mainly concerned with the thermodynamic stability of ASD but alone cannot govern the absolute stability of the ASD because it does not account the kinetic stability [124]. At room temperature as well, the positive ΔG_{mix} was showing the instability of all the compositions of drug-polymer. From equation 3.1 and 3.2, it can be seen that smaller the value of χ more negative will be the ΔG_{mix}, designating the drug-polymer complex to be more stable and a greater number of interactions between drug and polymer [197]. Therefore, positive values of χ obtained at 25 ^{o}C showed the formation of immiscible drug-polymer system (Table 3.5). The negative value of χ is obtained at <94 ^{o}C, <80 ^{o}C and <66 ^{o}C for RLZ-PAA, RLZ-PVP VA and RLZ-HPMC AS, respectively (Figure 3.16 a, b, and c). This highlights the temperature at which the drug-polymer system may exist as a homogenous phase. The value of interaction parameter was observed to be influenced by each factor encompassing Flory-Huggins model, thus could not be used for comparison between different drug-polymer systems [53]. So, the χ values for each drug-polymer system at 25 ^{o}C were not sufficient to conclude the grading of polymer in terms of its efficacy in complete amorphousization to give stable ASDs. Hence, the system was further evaluated by solubility and miscibility curves.

Table 3.5. Values of constant A, constant B and interaction parameter (χ) for three RLZ-polymer systems

S.No.	Drug-Polymer System	Constant A	Constant B	Interaction Parameter (χ)	
				at 25^{o}C	At melting point
1	RLZ-PAA	-210.73	77574	49.45	-12.83
2	RLZ-PVP VA	-45.08	16009	8.61	-4.24
3	RLZ-HPMC AS	-155.86	53012	21.94	-20.62

Henceforth, further insight to understand the potential of polymer towards formation of stable ASD was taken by preparing the phase diagram of miscibility temperature and solubility temperature (calculated using equation 3.4) *vs* drug volume fraction. This

information was paired with predicted T_g of the system with different weight ratios of drug and polymer, which were calculated using Gordon-Taylor equation (equation 3.5).

$$T_g = \frac{W_1 T_{g1} + K_G W_2 T_{g2}}{W_1 + K_G W_2} \quad \text{Equation 3.5}$$

Where T_g, T_{g1}, and T_{g2} are the glass transition temperatures of the drug-polymer mixture, drug in amorphous form and the polymer, respectively. The constant value K_G can be calculated using equation 3.6.

$$K_G = \frac{\rho_1 T_{g1}}{\rho_2 T_{g2}} \quad \text{Equation 3.6}$$

Where ρ1 and ρ2 are the true density value of amorphous drug and polymer, respectively. This phase diagram concerns the range of temperature and composition, below and above which the system exists in single-phase and two-phase thermodynamic region. Through phase diagram (Figure 3.16 a, b and c), information about the maximum solubility and miscibility of amorphous drug within the polymeric matrix and its dependence on temperature can be obtained. The region lying at the right-hand side of the spinodal T_g curve is considered as unstable where the drug-polymer exists in two phase heterogenous system. To the left-hand side exists the region on drug-polymer single-phase homogenous system. At the right-hand side of the T_g curve recrystallization of the drug can occur without any significant energy barrier. The solubility and the miscibility curve intersecting the predicted glass transition curve can be seen. Quantitative determination of miscibility of RLZ in PAA, PVP VA and HPMC AS was observed to be approximately 10% w/w at <85 ^oC, 25% w/w at <71 ^oC and 35% w/w at <61 ^oC, respectively. This revealed the extent of drug loading possible until these temperatures achieved which could result into a stable ASD of RLZ without rendering any sort of recrystallization. Additionally, in the case of PAA, and PVP VA at 50%w/w drug loading there is positive

deviation in the T_g value i.e., the observed value is higher than predicted. In case of HPMC AS at the same drug loading a negative deviation in the T_g value is observed. A positive deviation is the evidence of heteronuclear interaction which leads to enhanced stability. On the other hand, the negative deviation is the evidence of homonuclear interaction which has destabilizing effect [195]. From this, it can be concluded that PAA can offer high stability to RLZ over higher temperatures; however, drug loading will be low. PVP VA observed to offer higher drug loading among the three polymers with stability over moderate temperature. While HPMC AS can produce a stable ASD with the highest drug loading but observed to have temperature limited lower thermodynamic stability compared to PAA and PVP VA. However, low drug loading observed in case of PAA can be easily addressed by adjusting the ASDs amount as dose of RLZ was not very high (50mg taken orally twice daily). In addition, it may not result in any pill burden at the cost of its stability. This experimental methodology is based on the measurement of the dissolution of crystalline drug into polymeric matrix at high drug loading and temperature. In this method, data generated is extrapolated to lower temperatures, which is often argued to give overestimation or underestimation of miscibility of drug in polymer. Therefore, this study is backed up with other studies to give a multi-faceted understanding of the interaction of drug with the selected polymers. For instance, intermolecular interactions like the formation of H-bonds or ionic bonds (as discussed in earlier study) plays the key role in determining the capacity of polymer to prevent the drug present in the ASD to recrystallize. The evaluation of the results obtained from all the studies should be considered to generate evidences in grading of polymers according to their efficacy to produce a stable ASD. Present study revealed PAA as effective polymer based on all above studies conducted for grading of polymers for development of RLZ ASDs.

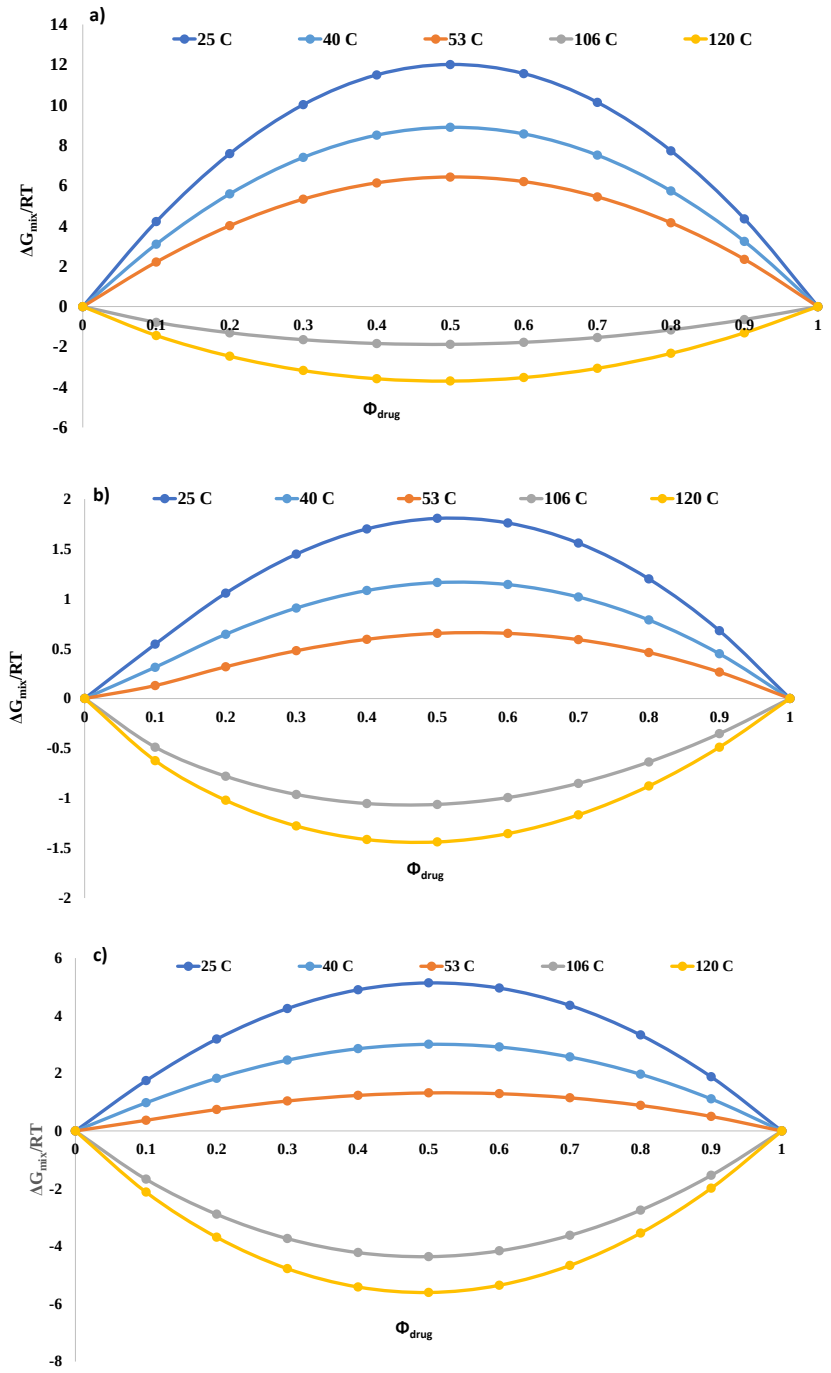

Figure 3.15. a) Plot of $\Delta G_{mix}/RT$ vs drug weight fraction (Φ_{drug}) for RLZ-PAA b) Plot of $\Delta G_{mix}/RT$ vs drug weight fraction (Φ_{drug}) for RLZ-PVP VA c) Plot of $\Delta G_{mix}/RT$ vs drug weight fraction (Φ_{drug}) for RLZ-HPMC AS

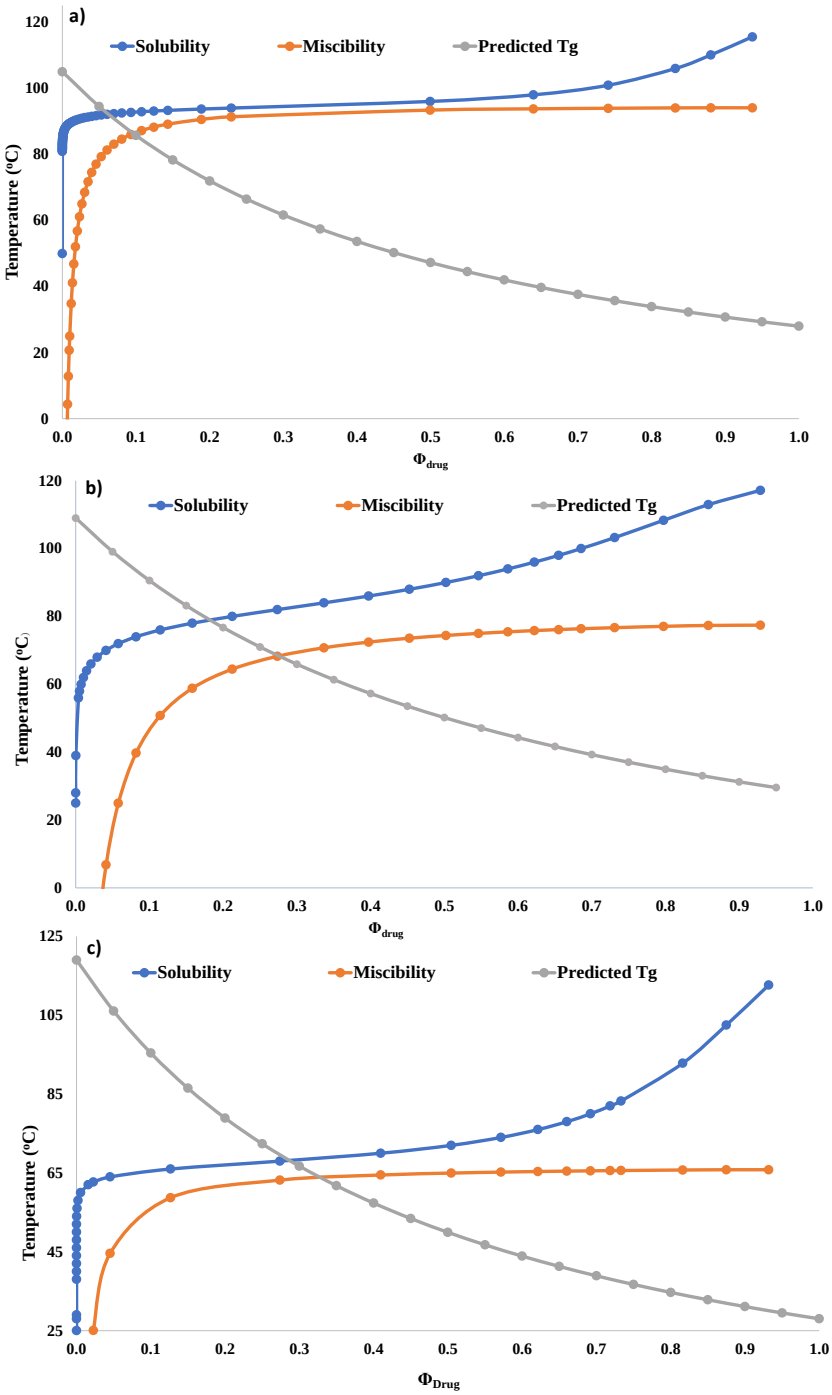

Figure 3.16. a) Binary phase diagram for RLZ-PAA b) Binary phase diagram for RLZ-PVP VA c) Binary phase diagram for RLZ-HPMC AS showing the solid liquid equilibrium (blue), miscibility (orange) and glass transition temperature (grey) curve

3.3.9 Long term stability studies

The stability data of all the three ASDs; RLZ:PAA, RLZ:PVP VA and RLZ-HPMC AS in the ratio 50:50 have been shown in figure 3.17. The XRD analysis of any sample at any time point did not show any difference. However, minor roughness in the halo peaks

were observed. This could be due to very small changes in ASD stability which is beyond the detection limit of XRD instrument. After 12 months no significant change in the XRD describes the suitability of all the three polymers for the preparation of ASD of RLZ.

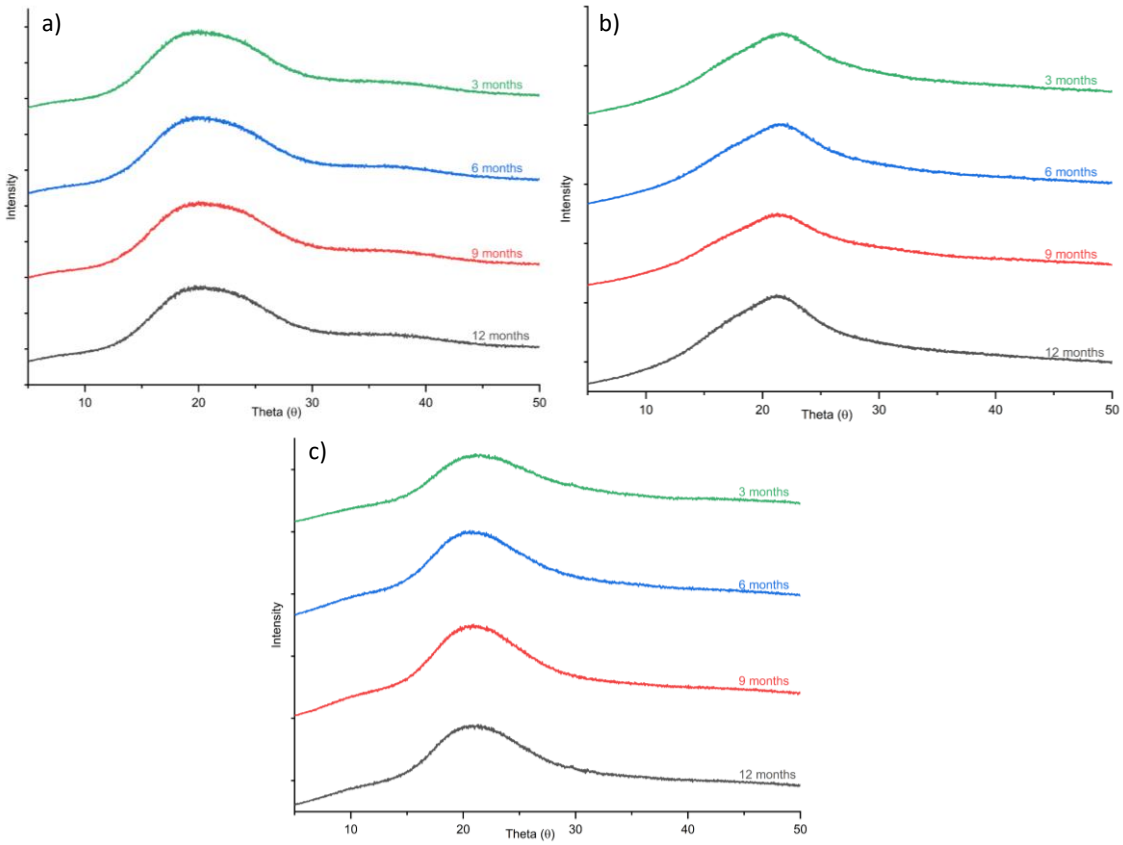

Figure 3.17. XRD patterns of stability samples of different time points of a) RLZ-PAA b) RLZ-PVP VA and c) RLZ-HPMC AS ASD

3.4 Conclusions

The current study provides a multi-pronged approach in deciding the use of most appropriate polymer according to its ability to provide stability to the ASD system. The initial screening of polymer done by molecular modeling and DFT studies, deciphered the mode of interactions between the drug and polymer along with the quantification of interactions in terms of energies. The XRD studies of the developed ASD with different drug and polymer ratios, revealed the capacity of polymer to stabilize a complete amorphous system. DSC thermogram showed the homogenous phase by exhibiting single

T_g for each ASD. In addition to this, *in situ* ASD preparation helped in determining the drug-polymer system giving the T_g value of 106 ^oC, 53 ^oC and 40 ^oC in 50:50 drug-polymer weight ratio, for ASD RLZ-PAA, RLZ-PVP VA and RLZ-HPMC AS respectively. This defines the capacity of polymers to increase the low T_g (28 ^oC) of pure amorphous RLZ, hence enhancing its stability. Chemical interaction studies with the help of FT-IR and ssNMR showed the formation of a molecular dispersion and the possible interactions occurring between the drug and polymer. Chemical stability was also confirmed using HPLC analysis. Assessment of crystallization tendency of the prepared ASDs indicated that PAA and PVP VA showed lower phase separation as the crystallization and fusion enthalpies were lower with respect to ASDs prepared with HPMC AS. This study evaluated the kinetic stability of ASDs prepared with different drug-polymer compositions. TEM studies were capable in detecting the presence of crystalline drug even in nanometer scale after it was exposed to high temperature, to ensure its thermodynamic stability. Additionally, *in vitro* dissolution study also showed superior dissolution capacity of RLZ:PAA ASD over other ASDs. The drug-polymer miscibility studies elaborated the stability space lying between the percent drug loading and the temperature. ΔG_{mix} of mixing at room, glass transition and melting temperatures of the drug-polymer systems were also taken into account. Hence, it can be inferred that PAA within its drug loading capacity would provide maximum stability to the RLZ ASD followed by PVP VA and HPMC AS. This multi-faceted approach will aid a faster and empirical selection of the most suitable polymer for the development of ASD which will be stable throughout its stipulated shelf-life. Even though these studies provide sufficient insight into the stability of ASDs, a real time stability study at accelerated conditions would provide exact results, which will be the future scope of this study. By exploiting

this approach industries can equip themselves to produce more such products; as till date, commercially available ASD products are very limited.